

VAGPO: Vision-augmented Asymmetric Group Preference Optimization for the Routing Problems

Shiyan Liu¹, Bohan Tan¹, Yan Jin¹

¹Department of Computer Science,
Huazhong University of Science and Technology,
Hubei, China

Abstract

The routing problems such as the Traveling Salesman Problem (TSP) and the Capacitated Vehicle Routing Problem (CVRP) are well-known combinatorial optimization challenges with broad practical relevance. Recent data-driven optimization methods have made significant progress, yet they often face limitations in training efficiency and generalization to large-scale instances. In this paper, we propose a novel Vision-Augmented Asymmetric Group Preference Optimization (VAGPO) approach for solving the routing problems. By leveraging ResNet-based visual encoding and Transformer-based sequential modeling, VAGPO captures both spatial structure and temporal dependencies. Furthermore, we introduce an asymmetric group preference optimization strategy that significantly accelerates convergence compared to commonly used policy gradient methods. Experimental results on TSP and CVRP benchmarks show that the proposed VAGPO not only achieves highly competitive solution quality but also exhibits strong generalization to larger instances (up to 1000 nodes) without re-training, highlighting its effectiveness in both learning efficiency and scalability.

Introduction

The Traveling Salesman Problem (TSP) and the Capacitated Vehicle Routing Problem (CVRP) are well-known routing problems with widespread applications in logistics, resource allocation, scheduling, and network design (Balducci, Bartolini, and Laporte 2010). They have been extensively studied in the operations research community and also frequently explored in artificial intelligence research. Due to their \mathcal{NP} -hard nature, traditional exact solvers such as Concorde (Applegate et al. 2006) become computationally infeasible for large-scale instances. As a result, numerous heuristic algorithms have been developed to efficiently obtain near-optimal solutions for practical applications.

In recent years, a soaring number of studies of data-driven optimization algorithms based on deep learning with supervised and reinforcement learning have been proposed to solve the routing problems. Most of these approaches treat the problems as a sequence generation task using the sequence-to-sequence architectures. They are typically categorized into two groups: constructive and iterative approaches. Constructive approaches incrementally generate a complete solution by adding one node at a time to a partial route. These approaches are highly efficient during inference, making

them well-suited for real-time applications, such as Attention Model (AM) (Kool, Van Hoof, and Welling 2018), PointerFormer (Jin et al. 2023), Policy Optimization with Multiple Optima (POMO) (Kwon et al. 2020), and its Preference Optimization (PO)-based version POMO+PO (Pan et al. 2025). In contrast, iterative approaches start from an initial solution and iteratively improve it through a neighborhood search based on certain local operators until a termination condition is met. These approaches, such as Wu et al. (2021), tend to be more computationally intensive during training and inference, but they often yield superior solution quality over time.

While most data-driven optimization algorithms focus on sequential representations, relatively few studies have explored structured representations that explicitly capture the spatial and topological properties of the routing problems. Graph Neural Networks (GNNs) (Scarselli et al. 2008) have been introduced to exploit the inherent graph structure of these problems, enabling the modeling of complex node relationships and topological features that are often challenging to capture with purely sequential models (Prates et al. 2019; Xing and Tu 2020). Most recently, vision-based approaches have emerged, where routing instances are encoded into image-like representations to exploit spatial patterns. These approaches leverage the observation that routing problems exhibit intrinsic spatial regularities, which can be effectively modeled using Convolutional Neural Networks (CNNs) (LeCun et al. 1989). For example, H-TSP (Pan et al. 2023) employs CNNs to process TSP instances as images, extracting spatial features that guide the optimization process.

In this paper, we propose a Vision-Augmented Asymmetric Group Preference Optimization (VAGPO) approach for solving the routing problems in a constructive manner. Built upon the classical encoder-decoder architecture (Vaswani et al. 2017), VAGPO incorporates a vision-based representation by transforming routing instances into image-like formats and utilizing a ResNet architecture (He et al. 2016) to extract both local and global spatial features. These features complement the sequential modeling capabilities of Transformer-based architectures, enabling improved spatial-temporal reasoning for trajectory generation.

The main contributions of our work are summarized as follows:

- We propose a cross-modal feature fusion mechanism that effectively integrates sequential and visual informa-

tion, enabling the model to jointly reason over temporal decision-making and spatial patterns by leveraging both local and global features.

- We introduce a reinforcement learning strategy, Asymmetric Group Preference Optimization (AGPO), which generalizes preference optimization to the multi-start node setting. By incorporating asymmetric optimization parameters and group-wise trajectory evaluations, AGPO improves training stability and convergence speed.
- The proposed VAGPO achieves highly competitive performance across all evaluated TSP and CVRP instances, while requiring substantially fewer training epochs than existing learning-based methods. And it can generalize well to instances that have varied distributions and scalability without re-training.

Related Work

We begin by highlighting several of the most prominent traditional algorithms for routing problems, followed by a focused discussion of recent data-driven optimization methods that are more closely related to our work.

Traditional approaches can be categorized into exact and heuristic methods. Concorde (Applegate et al. 2006) is one of the most well-known exact solvers, which formulates the problem using mixed integer programming and solves it through a branch-and-cut framework. LKH3 (Helsgaun 2017) and HGS (Vidal 2022) are SOTA heuristics using neighborhood search and a population-based framework to efficiently find high-quality solutions.

With the rapid progress of deep learning, data-driven optimization algorithms for routing problems have gained increasing attention. These methods are generally classified into constructive and iterative approaches. Constructive methods generate solutions incrementally by sequentially selecting nodes. Pointer Network (Vinyals, Fortunato, and Jaitly 2015) was the first to apply deep learning to combinatorial problems. Building on this, Bello et al. (2016) introduced a reinforcement learning (RL) framework that eliminates the need for optimal labels. Nazari et al. (2018) improved representation by mapping node features into a shared high-dimensional space. Inspired by Transformers (Vaswani et al. 2017), Kool, Van Hoof, and Welling (2018) proposed the AM, replacing RNNs in Seq2Seq structures with attention modules. Further developments include Multi-Decoder AM (Xin et al. 2021a) and POMO (Kwon et al. 2020), which leverage problem symmetries to enhance performance. While effective, POMO is limited by symmetry assumptions. Sym-NCO (Kim, Park, and Park 2022) generalizes symmetry-aware learning across broader tasks, and POMO+PO (Pan et al. 2025) further advances the field by integrating preference-based learning into state-of-the-art models. Pointerformer (Jin et al. 2023) improves the Transformer backbone, and Poppy (Grinsztajn et al. 2024) introduces diverse policy populations without relying on explicit sampling strategies.

In contrast, iterative approaches refine an initial solution through neighborhood search, combining traditional solvers with learning-based guidance. Lu, Zhang, and Yang (2019) integrated RL with LKH to control handcrafted improvement

rules. de O. Costa et al. (2020) and Sui et al. (2021) applied RL to guide 2-opt and 3-opt operators. NLNS (Hottung and Tierney 2020) merged RL with large neighborhood search (Shaw 1998). NeuroLKH (Xin et al. 2021b) used a supervised sparse graph network to generate candidate edge sets. SGBS (Choo et al. 2022) combined neural policy networks with simulation-based tree search, while Neural k -Opt (Ma, Cao, and Chee 2024) employed a dual-stream decoder and action factorization for adaptive exchanges.

Recently, diffusion models have emerged as promising alternatives. DIFUSCO (Sun and Yang 2023) and T2T (Li et al. 2023) apply diffusion-based generative techniques to solve complex combinatorial optimization problems, highlighting the potential of continuous generative models in discrete domains.

To overcome the limitations of sequential representations, researchers have explored structured methods that better capture geometric and topological properties. Among them, graph-based models have shown strong potential. Prates et al. (2019) demonstrated that GNNs (Scarselli et al. 2008) can solve NP-complete problems by integrating symbolic and numerical reasoning. GREAT (Xing and Tu 2020) further improved efficiency through edge sparsification while preserving key structural information.

Vision-based representations also offer a promising alternative. TSP (Pan et al. 2023) uses a hierarchical framework where CNNs (LeCun et al. 1989) encode TSP instances as images, capturing spatial relationships between nodes. These visual features reveal patterns often missed by sequence models. However, most vision-based methods lack effective integration with sequential processing, limiting their ability to jointly reason over spatial and temporal dependencies—an essential capability for high-quality routing solutions.

Problem Definition

In this paper, we focus on the routing problems in the Euclidean space, specifically the TSP and CVRP, which are the two most prevalent ones.

Traveling Salesman Problem Let $G = (V, E)$ denote an undirected graph, where V represents the set of N nodes and E represents the set of edges connecting these nodes. For each edge connecting nodes i and j , we define $cost(i, j)$ as the Euclidean distance between them. A special node $v_d \in V$ is designated as the depot where the route begins and ends. A feasible solution to a TSP instance is a Hamiltonian cycle that visits each node exactly once. Our objective is to minimize the total cost of the solution route τ , which can be calculated by Eq. (1), where v_i represents the i -th node in the route. All node coordinates are normalized to lie within $[0, 1]^2$.

$$L(\tau) = \sum_{i=1}^{N-1} cost(v_i, v_{i+1}) + cost(v_N, v_1) \quad (1)$$

Capacitated Vehicle Routing Problem Let $G = (V, E)$ denote an undirected graph with N nodes and associated edges. Each edge has a cost defined as the Euclidean distance between its endpoints. Node $v_d \in V$ serves as the depot. Each non-depot node, called the customer node, has an associated demand d . Each vehicle has a maximum capacity Q .

A feasible CVRP solution consists of a set of routes where: (1) each route starts and ends at the depot, (2) each non-depot node is visited exactly once by exactly one route, and (3) the total demand served by each route does not exceed Q . The objective is to minimize the total cost across all routes, can be calculated as in Eq. (2), where v_i^k is the i -th node in the k -th route, m_k is the number of nodes in that route, and $v_1^k = v_{m_k}^k = v_d$. All node coordinates are normalized to lie within $[0, 1]^2$.

$$L(\tau) = \sum_{k=1}^K \sum_{i=1}^{m_k-1} \text{cost}(v_i^k, v_{i+1}^k) \quad (2)$$

The Proposed VAGPO Approach

The proposed VAGPO approach is a constructive algorithm based on the Transformer architecture (Vaswani et al. 2017), which combines a cross-modal encoder and an auto-regressive decoder to generate high-quality solutions for the routing problems. The general framework of VAGPO is illustrated in Figure 1.

In principle, VAGPO employs a vision representation that transforms node coordinates into an image-like format and uses the ResNet (He et al. 2016) architecture to extract both local and global visual features, effectively capturing the geometric relationships among nodes. These visual features are then integrated with sequential information via a cross-modal feature fusion mechanism, which combines the spatial representations extracted by CNNs (LeCun et al. 1989) with the sequence modeling capabilities of a Transformer encoder. The resulting node embeddings are passed to an auto-regressive decoder, which constructs the routing solution by selecting one node at a time based on the learned probability distribution. To improve training efficiency, VAGPO is trained using a reinforcement learning strategy AGPO, which extends preference-based learning to a multi-start setting. This training paradigm allows for diverse trajectory evaluation and policy refinement.

Vision Representation

To better capture the spatial structure inherent of TSP and CVRP, VAGPO begins by transforming each problem instance into an image-like representation. This transformation encodes the spatial layout of nodes in a format amenable to convolutional processing. To extract meaningful spatial features, we adopt a CNN-based encoder, specifically leveraging the ResNet architecture. This encoder is designed to learn both global contextual features of the instance and local geometric patterns surrounding each node, thereby enriching the encoder’s embedding of spatial dependencies crucial for effective routing generation.

For the TSP, we convert the set of node coordinates $\{(x_i, y_i)\}_{i=1}^N$, where N is the number of nodes and (x_i, y_i) denotes the normalized 2D coordinate of node v_i , into a fixed-size grayscale image of 224×224 . Each node v_i is mapped to its corresponding pixel location (x_i, y_i) , where the pixel value is set to 1 at the node’s location and 0 elsewhere. The resulting image is then duplicated across three channels to form a $224 \times 224 \times 3$ image. Given that N is much smaller

than the number of pixels M , the probability that at most one pixel contains multiple nodes can be approximated using the binomial formula:

$$P \approx (1 - p)^M + Mp(1 - p)^{M-1}, \quad (3)$$

where p is the probability that a pixel contains multiple nodes:

$$p = 1 - e^{-\frac{N}{M}} - \frac{N}{M}e^{-\frac{N}{M}} \quad (4)$$

For $N = 100$ and $M = 224 \times 224$, this probability exceeds 99%, indicating that the impact of node collisions is negligible in practice.

For the CVRP, we convert the nodes into a three-channel image to distinguish different node types and encode demand information, where d_j denotes the normalized demand of customer node v_j . Specifically, let $P_{(x,y)} = [c_1, c_2, c_3]$ denote the value of the three channels at pixel (x, y) , where (x, y) is a pixel position in the image. The channel values are defined as:

$$P_{(x,y)} = \begin{cases} [1, 1, 0], & \text{if depot } v_d \text{ at } (x, y) \\ [1, 0, d_j], & \text{if customer } v_j \neq v_d \text{ at } (x, y) \\ [0, 0, 0], & \text{otherwise} \end{cases} \quad (5)$$

In this way, we have shifted the problem representation from numerical to visual. After this, we use a pretrained and frozen ResNet-18 as the image encoder to extract the feature map $G \in \mathbb{R}^{B \times C \times H \times W}$, where B is the batch size, C is the number of channels, and H, W are the height and width of the feature map, respectively. To fully utilize the global and local features, we first perform adaptive average pooling on the feature map G and then obtain the feature embedding F_i for node v_i by bilinear interpolation according to its normalized coordinates (x_i, y_i) . Finally, the embedding F'_i of v_i consists of a combination of G , F_i , and the positional encoding P_i of v_i , as shown in Eq.(6) and Eq.(7), where

$$P_i = \text{Linear}([x_i, y_i]) \quad (6)$$

$$F'_i = \text{Linear}(G \oplus F_i \oplus P_i) \quad (7)$$

After the projection, the resulting $F'_i \in \mathbb{R}^{B \times D}$, where D is the embedding dimension, possesses the same shape as the output of the Transformer encoder, thereby facilitating seamless integration in the subsequent cross-modal feature fusion stage. Despite the inevitable information loss introduced by visual encoding, its inherent locality serves as a valuable complement to the global modeling capacity of sequential information. The specific fusion strategy will be detailed in the next section.

Cross-modal Feature Fusion

To effectively integrate both spatial and sequential information in routing problems, we design a cross-modal feature fusion module within the encoder-decoder framework. While the Transformer architecture remains the backbone for modeling sequential dependencies, we incorporate visual features extracted from the image-based representation to enhance spatial awareness. By aligning the sequential and visual feature tensors into a common embedding space, the fusion

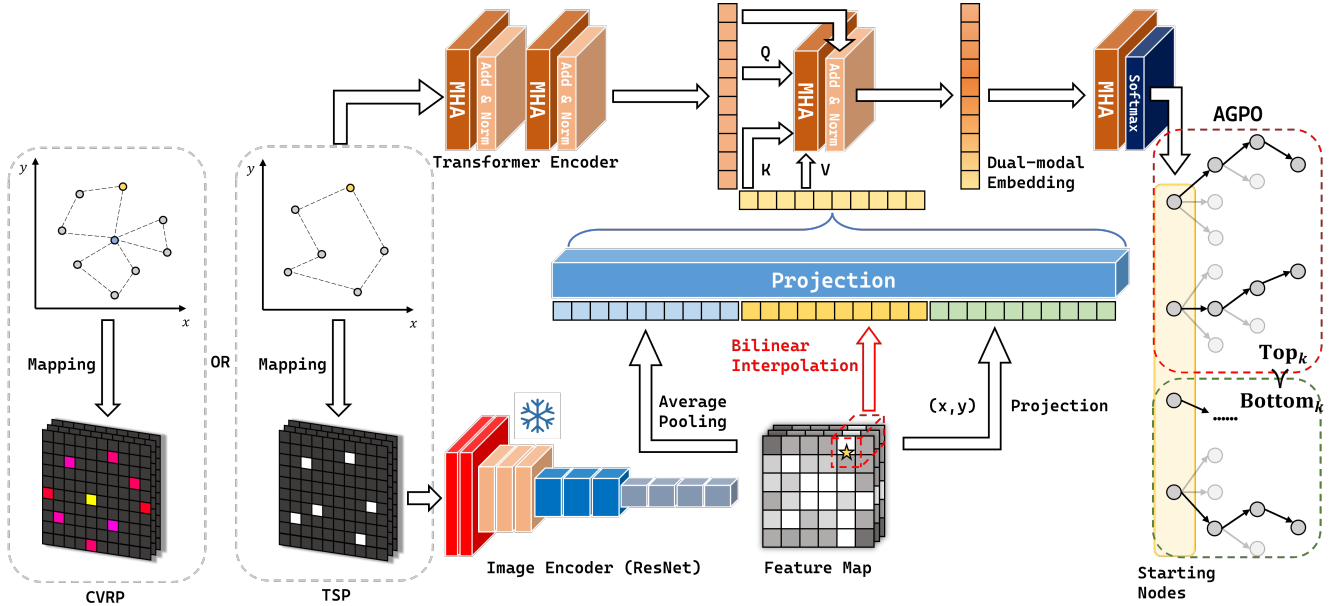


Figure 1: The overall framework of the proposed VAGPO approach

mechanism enables the model to jointly reason over spatial structures and routing sequences, unlocking complementary strengths from both modalities.

Since both the sequential and visual features are preprocessed into tensors of the same dimensionality, the fusion network, mainly populated by a multi-head attention (MHA) layer and a feed forward (FF) layer, is adopted along with residual connections. By enabling each node in the sequential feature space to attend to multiple subspaces of the visual modality, the multi-head attention mechanism allows the model to capture diverse and complementary cross-modal information, thus enhancing the effectiveness of feature fusion. Let $T \in \mathbb{R}^{B \times N \times D}$ denote the sequential features obtained from the Transformer encoder and $V \in \mathbb{R}^{B \times N \times D}$ denote the visual features extracted from the ResNet encoder. The fused features F are computed as in Eq. (8).

$$F = T + \alpha_1 \cdot \text{MHA}_{T \rightarrow V}(T, V) + \alpha_2 \cdot \text{FF}(T + \alpha_1 \cdot \text{MHA}_{T \rightarrow V}(T, V)) \quad (8)$$

Here, α_1 and α_2 are learnable scaling factors, and $\text{FF}(\cdot)$ denotes a feed-forward layer.

Specifically, $\text{MHA}_{T \rightarrow V}$ refers to a multi-head attention mechanism where sequential features T act as queries (Q) and visual features V serve as keys and values (K, V). For a single attention head:

$$\text{Attention}(T, V) = \text{softmax} \left(\frac{(W_q T)(W_k V)^T}{\sqrt{D}} \cdot \beta \right) (W_v V) \quad (9)$$

where $W_q, W_k, W_v \in \mathbb{R}^{D \times D}$ are learnable projection matrices and β is a learnable scaling factor. In the multi-head case, the outputs of H attention heads, each with independent projection parameters, are concatenated and mapped by $W_o \in \mathbb{R}^{D \times D}$:

$$\text{MHA}_{T \rightarrow V}(T, V) = W_o[\text{head}_1; \dots; \text{head}_H] \quad (10)$$

Each head_h is computed as in Eq. (9).

One notices that this hierarchical information fusion mechanism and multiple residual connections are used, which are capable of mitigating gradient vanishing during training while exhibiting strong representational ability.

Asymmetric Group Preference Optimization

Addressing the twin challenges of high variance and low sample utilization in policy gradient methods for routing, preference optimization (PO) approaches such as POMO+PO (Pan et al. 2025) offer a promising alternative by replacing quantitative losses with qualitative comparisons through the Bradley-Terry (BT) model (Bradley and Terry 1952), thus establishing a preference-based mechanism for combinatorial optimization. Despite this conceptual shift, the underlying on-policy REINFORCE framework constrains their sample efficiency. We propose a reinforcement learning strategy, AGPO, designed to maximize the benefits of BT-model-based preference learning. AGPO explicitly compares the relative quality within groups of solution trajectories. This formulation enables fundamentally more stable optimization and unlocks significantly higher learning efficiency and sample utilization compared to existing preference-based methods.

Given a sequence of starting nodes from V that generate corresponding trajectories $\tau' = (\tau^1, \tau^2, \dots, \tau^n)$, and assuming these trajectories have rewards in descending order $r_{\tau^1} > r_{\tau^2} > \dots > r_{\tau^n}$, we can formally obtain preference pairs $D(r_{\tau^i}, r_{\tau^j})$ where $i < j$. For all samples, the joint likelihood is:

$$J(\theta) = \prod_{i < j} P(r_{\tau^i} \succ r_{\tau^j} | V) \quad (11)$$

To facilitate optimization, we take the logarithm of the joint

likelihood and add a negative sign to obtain the loss function:

$$L(\theta) = - \sum_{i < j} \log P(r_{\tau^i} \succ r_{\tau^j} | V) \quad (12)$$

Substituting the BT formula as in PO, we get:

$$\begin{aligned} L(\theta) &= - \sum_{i < j} \log \left(\frac{\exp(r_{\tau^i})}{\exp(r_{\tau^i}) + \exp(r_{\tau^j})} \right) \\ &= - \sum_{i < j} [\log \sigma(r_{\tau^i} - r_{\tau^j})] \end{aligned} \quad (13)$$

Following the approach in Direct Preference Optimization (DPO) (Rafailov et al. 2023), we parameterize the reward function as the difference in log probabilities between the current policy and a reference policy:

$$r(x, y) = \beta \log \frac{\pi_\theta(\tau|V)}{\pi_{\text{ref}}(\tau|V)} \quad (14)$$

For routing problems, departing from the depot, not every starting node leads to optimal solutions, which is particularly evident in CVRP where the quality of solutions can vary significantly depending on the starting node. To address this challenge within the multi-start nodes, we introduce an innovative grouping strategy to improve robustness.

Rather than considering preferences between individual trajectories, which can be unstable during training, we partition the trajectories into high-quality and low-quality groups. Specifically, we unify the probabilities of the top k trajectories $\prod_{i=1}^k \pi_\theta(\tau^i)$ as a group optimal probability, and similarly consolidate the probabilities of the bottom k trajectories $\prod_{j=n-k+1}^n \pi_\theta(\tau^j)$ as a group suboptimal probability. This grouping approach creates more robust probability pairs, reducing sensitivity to individual trajectory variations and improving training stability. The reward function for our grouped trajectories becomes:

$$r(x, y) = \beta \log \prod_i \frac{\pi_\theta(\tau^i|V)}{\pi_{\text{ref}}(\tau^i|V)} \quad (15)$$

We further establish asymmetric coefficients ($\beta_w > \beta_l$) to place greater emphasis on improving the quality of positive samples. Here, τ_{pref} and τ_{nonpref} indicate the groups of highest and lowest reward trajectories, respectively:

$$r_w(x, y) = \beta_w \log \frac{\pi_\theta(\tau_{\text{pref}}|V)}{\pi_{\text{ref}}(\tau_{\text{pref}}|V)} \quad (16)$$

$$r_l(x, y) = \beta_l \log \frac{\pi_\theta(\tau_{\text{nonpref}}|V)}{\pi_{\text{ref}}(\tau_{\text{nonpref}}|V)} \quad (17)$$

This asymmetric weighting allows the model to focus more on improving promising solutions while maintaining a suitable learning signal from suboptimal trajectories. The training process of AGPO is presented in Algorithm 1. It begins with policy initialization, followed by iterative collection of reference trajectories, identification of preferred and non-preferred groups, and policy updates through the asymmetric preference optimization approach.

Algorithm 1: The AGPO Training

Input: Training set S , number of starting nodes per sample N , number of total training steps T , batch size B

Output: Optimized policy π_θ

Initialize policy network π_θ ;

for $step = 1$ **to** T **do**

 Collect trajectories $\{\tau_{\text{ref}}^i\}_{i=1}^B$ using π_θ ;

 Compute rewards $R(\tau_{\text{ref}}^i)$ and memories M_{ref}^i ;

 Select top- k trajectories: $\{\tau_{\text{pref}}^i\} \leftarrow \text{Top}_k(R(\tau_{\text{ref}}^i))$;

 Select bottom- k trajectories:

$\{\tau_{\text{nonpref}}^i\} \leftarrow \text{Bottom}_k(R(\tau_{\text{ref}}^i))$;

for $iteration = 1$ **to** K **do**

 Collect trajectories $\{\tau_{\text{curr}}^i\}_{i=1}^B$ using π_θ ;

 Compute log-probability ratios:

$\log \prod_i \frac{\pi_\theta(\tau_{\text{pref}}^i)}{\pi_{\text{ref}}(\tau_{\text{pref}}^i)}$ and $\log \prod_j \frac{\pi_\theta(\tau_{\text{nonpref}}^j)}{\pi_{\text{ref}}(\tau_{\text{nonpref}}^j)}$;

 Formulate the loss function:

$\mathcal{L}_{\text{AGPO}} = -\mathbb{E} [\log \sigma(\beta_w \Delta_{\text{pref}} - \beta_l \Delta_{\text{nonpref}})]$;

 Update parameters: $\theta \leftarrow \theta - \alpha \nabla_\theta \mathcal{L}_{\text{AGPO}}$;

return Optimized policy π_θ

Experimental Results

Baselines We compare our VAGPO against a number of leading baselines, including the exact solver Concorde (Applegate et al. 2006), the heuristic algorithm LKH3 (Helsgaun 2017), and several deep reinforcement learning models such as AM (Kool, Van Hoof, and Welling 2018), POMO (Kwon et al. 2020), and Pointerformer (Jin et al. 2023). We also include recent SOTA algorithms like DIFUSCO (Sun and Yang 2023) and POMO+PO (Pan et al. 2025).

Training For all experiments, training used a single RTX 4090 GPU with a batch size of 64. Adam optimizer is used with a learning rate $\eta = 10^{-4}$ and a weight decay $w = 10^{-6}$. For AGPO, we set $\beta_w = 0.5$, $\beta_l = 0.1$, $\text{Top}_k = 10$.

To strike a balance between efficiency and effectiveness in spatial representation learning, we chose ResNet-18 (He et al. 2016) as our lightweight backbone, instead of more complex alternatives such as ResNet-50, Vision Transformer (ViT) (Dosovitskiy et al. 2020), or GNNs (Scarselli et al. 2008). An epoch is defined as training across 100,000 randomly generated instances. Despite introducing only minor computational overhead, our method completes a full training epoch in under 13 minutes. For reference, under the same experimental conditions, POMO requires 5 minutes per epoch, and POMO+PO takes 9 minutes per epoch.

Inference We follow the convention and report the time for solving 10,000 random instances of each problem. Similar to POMO, we have also performed inferences with $\times 8$ instance augmentation, which has long been recognized as an effective post-processing technique.

We conduct training and evaluation on TSP instances with 50 and 100 nodes, and assess generalization by testing the trained models on larger instances with 500 and 1000 nodes. Table 1 presents the quantitative results, comparing

our method with existing baselines. Performance is evaluated using three metrics: length (total tour cost), gap (optimality gap w.r.t. Concorde), and time (inference efficiency). The optimal solutions for the test sets are computed using Concorde.

As shown in Table 1, VAGPO consistently outperforms POMO and POMO+PO, achieving smaller optimality gaps with only a modest increase in inference time. Compared to SOTA methods such as DIFUSCO, VAGPO offers a superior solution quality while maintaining lower inference latency. Moreover, our approach exhibits the shortest training time among all baselines, highlighting its strong trade-off between learning efficiency and solution accuracy.

To assess generalization, we evaluate models trained on TSP-50 and TSP-100 directly on larger instances. As shown in Table 2, VAGPO maintains competitive solution quality and consistently outperforms POMO. This demonstrates that our approach combines low training cost with efficient inference, enabling scalable optimization without significant computational overhead.

Figure 2 shows the training curves of various methods on TSP-100, highlighting the efficiency and stability of our learning process. Notably, VAGPO converges to competitive performance within just one-tenth of the training epochs required by POMO, demonstrating significantly improved learning efficiency. While some baselines achieve marginally better final results, they do so at substantially higher training costs. In contrast, VAGPO offers excellent cost-effectiveness, making it particularly well-suited for resource-constrained and latency-sensitive applications.

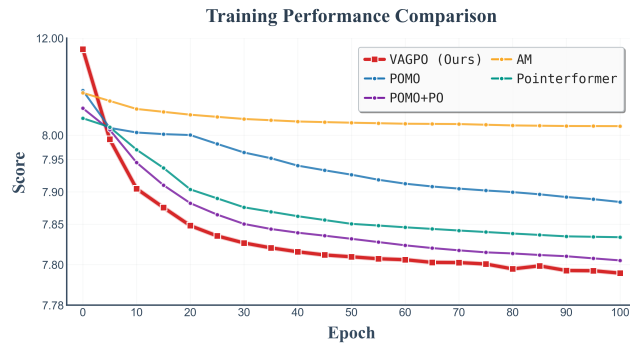


Figure 2: Training performance among different methods

Following the strong performance of our model on TSP, we further evaluate its effectiveness on the CVRP across various scales. As reported in Table 3, VAGPO achieves near-optimal results on CVRP instances with 20, 50, and 100, with performance measured relative to the leading heuristic LKH3. Note that the results of 500 nodes are obtained using models trained on 100-node instances to test generalization. Notably, no known algorithm can solve 10,000-instance CVRP sets to optimality within a reasonable timeframe. In this context, our approach matches or exceeds the performance of recent SOTA methods, offering competitive solution quality and computational efficiency in both training and inference.

Ablation Study

To rigorously assess our design choices, we conducted ablation studies summarized in Table 4 and visualized in Figure 3. The training curves highlight the cumulative benefits of our architectural components, with the full model achieving high-quality solutions approximately 30% faster than all ablated variants. Each component demonstrably contributes to improved performance, yielding faster convergence and better solution quality across diverse instances. On TSP-100, the systematic evaluation reveals clear performance gains attributable to each design element, underscoring the overall effectiveness of our approach.

Table 4: Ablation study configurations on TSP-100. Variants 1–4 test a single component. Variants 5–6 examine different vision encoder settings. Variants 7–9 explore various AGPO parameter configurations.

Exp.	Backbone	Frozen	AGPO Params		
			β_w	β_l	Top _k
Variant 1	\times	N/A	0.5	0.1	10
Variant 2	ViT	✓	N/A	N/A	N/A
Variant 3	GNNs	✓	N/A	N/A	N/A
Variant 4	ResNet-18	✓	N/A	N/A	N/A
Variant 5	ResNet-18	\times	0.5	0.1	10
Variant 6	ResNet-50	✓	0.5	0.1	10
Variant 7	ResNet-18	✓	0.5	0.5	10
Variant 8	ResNet-18	✓	0.5	0.1	1
Variant 9	ResNet-18	✓	0.5	0.1	50
VAGPO	ResNet-18	✓	0.5	0.1	10

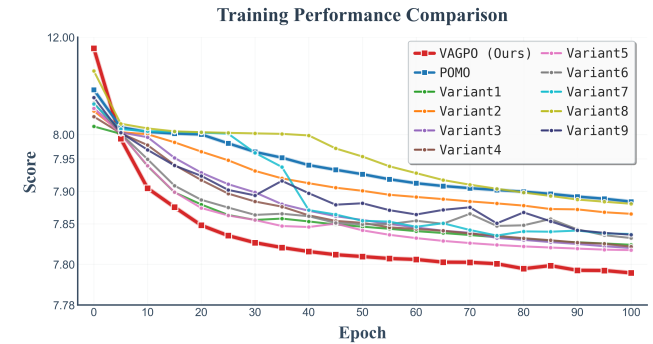


Figure 3: Training performance on VAGPO and variants

Backbone The backbone serves as a spatial feature extractor. Compared to GNNs (Scarselli et al. 2008) ($\sim 2\times$ slower) and ViT (Dosovitskiy et al. 2020) ($\sim 4\times$ slower) in training, which mainly provide global information already covered by the attention mechanism, ResNet (He et al. 2016) supplements local spatial details and reduces potential information loss. Notably, ResNet-18 is more suitable than complex networks like ResNet-50 for extracting features from sparse visual representations, capturing essential spatial relationships without unnecessary computational overhead. Freezing pre-trained weights eliminates complex parameter

Table 1: Experimental results on the TSP instances

Method	Type	TSP-50			TSP-100		
		Len.	Gap	Time	Len.	Gap	Time
Concorde	Exact	5.69	0.00%	(13m)	7.76	0.00%	(1h)
LKH3	OR	5.69	0.00%	(6m)	7.76	0.00%	(25m)
Gurobi	OR	5.69	0.00%	(2m)	7.76	0.00%	(17m)
OR Tools	OR	5.85	2.87%	(5m)	8.06	3.86%	(23m)
POMO, no augment.	RL+AS	5.70	0.12%	(2s)	7.80	0.46%	(11s)
POMO, $\times 8$ augment.	RL+AS	5.69	0.03%	(16s)	7.77	0.15%	(1.0m)
Pointerformer	RL	5.69	0.02%	(12s)	7.77	0.15%	(1m)
DIFUSCO	SL+G	5.71	0.45%	(9m)	7.85	1.21%	(9m)
DIFUSCO	SL+S	5.69	0.09%	-	7.78	0.23%	-
POMO+PO, $\times 8$ augment.	PO+AS	5.69	0.02%	(16s)	7.76	0.07%	(1.0m)
VAGPO, no augment.	PO+AS	5.69	0.05%	(13s)	7.78	0.25%	(17s)
VAGPO, $\times 8$ augment.	PO+AS	5.69	0.01%	(1.0m)	7.76	0.03%	(2.2m)

Table 2: Generalization results on TSP instances where POMO and VAGPO use $\times 8$ augmentation. "Size N " refers to the corresponding models trained on the instances with N nodes.

Method	TSP-50			TSP-100			TSP-500			TSP-1000		
	Len.	Gap	Time	Len.	Gap	Time	Len.	Gap	Time	Len.	Gap	Time
Concorde	5.69	0.00%	(13m)	7.76	0.00%	(1h)	16.55	0.00%	(4h)	23.12	0.00%	(7h)
LKH3	5.69	0.00%	(6m)	7.76	0.00%	(25m)	16.55	0.00%	(46m)	23.12	0.00%	(3h)
GCN	-	-	-	-	-	-	29.72	79.61%	(7m)	48.62	110.29%	(29m)
POMO, size 50	5.69	0.03%	(16s)	7.81	0.69%	(1.0m)	21.65	30.82%	(1.5h)	33.52	44.98%	(11.6h)
POMO, size 100	5.69	0.07%	(16s)	7.77	0.14%	(1.0m)	19.49	17.76%	(1.5h)	30.71	32.82%	(11.6h)
VAGPO, size 50	5.69	0.01%	(1.0m)	7.78	0.30%	(2.2m)	22.47	35.77%	(2.8h)	33.95	46.86%	(21.8h)
VAGPO, size 100	5.69	0.02%	(1.0m)	7.76	0.03%	(2.2m)	18.71	13.09%	(2.8h)	28.92	25.08%	(21.8h)

Table 3: Experimental results on the CVRP instances.

Method	CVRP-20			CVRP-50			CVRP-100			CVRP-500		
	Len.	Gap	Time	Len.	Gap	Time	Len.	Gap	Time	Len.	Gap	Time
LKH3	6.12	0.00%	(2h)	10.38	0.00%	(7h)	15.68	0.00%	(12h)	40.06	0.00%	(48h)
OR Tools	6.42	4.84%	(2m)	11.22	8.12%	(12m)	17.14	9.34%	(1h)	-	-	-
POMO, no augment.	6.17	0.82%	(1s)	10.49	1.14%	(4s)	15.83	0.98%	(9s)	48.34	20.64%	(13.1m)
POMO, $\times 8$ augment.	6.14	0.21%	(5s)	10.42	0.45%	(26s)	15.73	0.32%	(1.2m)	44.81	11.85%	(1.8h)
VAGPO, no augment.	6.14	0.32%	(3s)	10.48	0.96%	(5s)	15.81	0.82%	(11s)	46.88	17.02%	(15.8m)
VAGPO, $\times 8$ augment.	6.12	0.05%	(23s)	10.42	0.38%	(35s)	15.72	0.25%	(1.5m)	44.25	10.46%	(2.1h)

updates and enhances training efficiency. This design choice is crucial during early optimization phases, enabling more robust node representation learning.

AGPO's Parameters Our optimized AGPO configuration employs asymmetric coefficients that emphasize improved positive sample quality, which is particularly valuable for complex problems where optimal starting nodes cannot be guaranteed. Hence, we implement Top- k to improve sample utilization efficiency and accelerate preference ratio calculations. It is evident that moderate values of k yield optimal performance, whereas smaller values reduce utilization efficiency and larger values sacrifice diversity through excessive selectivity. This optimized approach consistently reduces required training iterations compared to baseline settings while producing shorter route lengths across test instances.

Conclusion

In this paper, we have introduced VAGPO, integrating visual representations with sequential processing for routing problems. By transforming routing instances into image-like formats and utilizing a cross-modal fusion mechanism, our approach effectively captures both spatial relationships and sequential dependencies. The proposed AGPO training strategy significantly improves convergence speed through asymmetric optimization parameters and group-based trajectory evaluation. Experimental results demonstrate that VAGPO achieves competitive performance on TSP and CVRP while requiring fewer training epochs, showing strong generalization to larger instances. This balance of solution quality and computational efficiency makes VAGPO particularly valuable for practical applications. Future work could explore more sophisticated visual encoders and extensions to other

combinatorial problems with inherent spatial structures.

References

Applegate, D.; Bixby, R.; Chvatal, V.; and Cook, W. 2006. Concorde TSP solver.

Baldacci, R.; Bartolini, E.; and Laporte, G. 2010. Some applications of the generalized vehicle routing problem. *Journal of the operational research society*, 61(7): 1072–1077.

Bello, I.; Pham, H.; Le, Q. V.; Norouzi, M.; and Bengio, S. 2016. Neural combinatorial optimization with reinforcement learning. *arXiv preprint arXiv:1611.09940*.

Bradley, R. A.; and Terry, M. E. 1952. Rank analysis of incomplete block designs: I. The method of paired comparisons. *Biometrika*, 39(3/4): 324–345.

Choo, J.; Kwon, Y.-D.; Kim, J.; Jae, J.; Hottung, A.; Tierney, K.; and Gwon, Y. 2022. Simulation-guided beam search for neural combinatorial optimization. *Advances in Neural Information Processing Systems*, 35: 8760–8772.

de O. Costa, P. R.; Rhuggenaath, J.; Zhang, Y.; and Akcay, A. 2020. Learning 2-opt heuristics for the traveling salesman problem via deep reinforcement learning. In *Asian Conference on Machine Learning*, 465–480. PMLR.

Dosovitskiy, A.; Beyer, L.; Kolesnikov, A.; Weissenborn, D.; Zhai, X.; Unterthiner, T.; Dehghani, M.; Minderer, M.; Heigold, G.; Gelly, S.; et al. 2020. An image is worth 16x16 words: Transformers for image recognition at scale. *arXiv preprint arXiv:2010.11929*.

Grinsztajn, N.; Furelos-Blanco, D.; Surana, S.; Bonnet, C.; and Barrett, T. 2024. Winner Takes It All: Training Performant RL Populations for Combinatorial Optimization. *Advances in Neural Information Processing Systems*, 36.

He, K.; Zhang, X.; Ren, S.; and Sun, J. 2016. Deep residual learning for image recognition. In *Proceedings of the IEEE conference on computer vision and pattern recognition*, 770–778.

Helsgaun, K. 2017. An extension of the Lin-Kernighan-Helsgaun TSP solver for constrained traveling salesman and vehicle routing problems. *Roskilde: Roskilde University*, 12: 966–980.

Hottung, A.; and Tierney, K. 2020. Neural Large Neighborhood Search for the Capacitated Vehicle Routing Problem. In *ECAI 2020*, 443–450. IOS Press.

Jin, Y.; Ding, Y.; Pan, X.; He, K.; Zhao, L.; Qin, T.; Song, L.; and Bian, J. 2023. Pointerformer: Deep reinforced multi-pointer transformer for the traveling salesman problem. In *Proceedings of the AAAI Conference on Artificial Intelligence*, volume 37, 8132–8140.

Kim, M.; Park, J.; and Park, J. 2022. Sym-nco: Leveraging symmetry for neural combinatorial optimization. *Advances in Neural Information Processing Systems*, 35: 1936–1949.

Kool, W.; Van Hoof, H.; and Welling, M. 2018. Attention, learn to solve routing problems! *arXiv preprint arXiv:1803.08475*.

Kwon, Y.-D.; Choo, J.; Kim, B.; Yoon, I.; Gwon, Y.; and Min, S. 2020. Pomo: Policy optimization with multiple optima for reinforcement learning. *Advances in Neural Information Processing Systems*, 33: 21188–21198.

LeCun, Y.; Boser, B.; Denker, J. S.; Henderson, D.; Howard, R. E.; Hubbard, W.; and Jackel, L. D. 1989. Backpropagation applied to handwritten zip code recognition. *Neural computation*, 1(4): 541–551.

Li, Y.; Guo, J.; Wang, R.; and Yan, J. 2023. T2t: From distribution learning in training to gradient search in testing for combinatorial optimization. *Advances in Neural Information Processing Systems*, 36: 50020–50040.

Lu, H.; Zhang, X.; and Yang, S. 2019. A learning-based iterative method for solving vehicle routing problems. In *International Conference on Learning Representations*.

Ma, Y.; Cao, Z.; and Chee, Y. M. 2024. Learning to search feasible and infeasible regions of routing problems with flexible neural k-opt. *Advances in Neural Information Processing Systems*, 36.

Nazari, M.; Oroojlooy, A.; Snyder, L.; and Takáć, M. 2018. Reinforcement learning for solving the vehicle routing problem. *Advances in Neural Information Processing Systems*, 31.

Pan, M.; Lin, G.; Luo, Y.-W.; Zhu, B.; Dai, Z.; Sun, L.; and Yuan, C. 2025. Preference Optimization for Combinatorial Optimization Problems. *arXiv preprint arXiv:2505.08735*.

Pan, X.; Jin, Y.; Ding, Y.; Feng, M.; Zhao, L.; Song, L.; and Bian, J. 2023. H-tsp: Hierarchically solving the large-scale traveling salesman problem. In *Proceedings of the AAAI Conference on Artificial Intelligence*, volume 37, 9345–9353.

Prates, M.; Avelar, P. H.; Lemos, H.; Lamb, L. C.; and Vardi, M. Y. 2019. Learning to solve np-complete problems: A graph neural network for decision tsp. In *Proceedings of the AAAI conference on artificial intelligence*, volume 33, 4731–4738.

Rafailov, R.; Sharma, A.; Mitchell, E.; Manning, C. D.; Ermon, S.; and Finn, C. 2023. Direct preference optimization: Your language model is secretly a reward model. *Advances in Neural Information Processing Systems*, 36: 53728–53741.

Scarselli, F.; Gori, M.; Tsoi, A. C.; Hagenbuchner, M.; and Monfardini, G. 2008. The graph neural network model. *IEEE transactions on neural networks*, 20(1): 61–80.

Shaw, P. 1998. Using constraint programming and local search methods to solve vehicle routing problems. In *International Conference on Principles and Practice of Constraint Programming*, 417–431. Springer.

Sui, J.; Ding, S.; Liu, R.; Xu, L.; and Bu, D. 2021. Learning 3-opt heuristics for traveling salesman problem via deep reinforcement learning. In *Asian Conference on Machine Learning*, 1301–1316. PMLR.

Sun, Z.; and Yang, Y. 2023. Difusco: Graph-based diffusion solvers for combinatorial optimization. *Advances in neural information processing systems*, 36: 3706–3731.

Vaswani, A.; Shazeer, N.; Parmar, N.; Uszkoreit, J.; Jones, L.; Gomez, A. N.; Kaiser, L.; and Polosukhin, I. 2017. Attention is all you need. *Advances in neural information processing systems*, 30.

Vidal, T. 2022. Hybrid genetic search for the CVRP: Open-source implementation and SWAP* neighborhood. *Computers & Operations Research*, 140: 105643.

Vinyals, O.; Fortunato, M.; and Jaitly, N. 2015. Pointer networks. *Advances in Neural Information Processing Systems*, 28.

Wu, Y.; Song, W.; Cao, Z.; Zhang, J.; and Lim, A. 2021. Learning improvement heuristics for solving routing problems. *IEEE transactions on neural networks and learning systems*, 33(9): 5057–5069.

Xin, L.; Song, W.; Cao, Z.; and Zhang, J. 2021a. Multi-decoder attention model with embedding glimpse for solving vehicle routing problems. In *Proceedings of the AAAI Conference on Artificial Intelligence*, volume 35, 12042–12049.

Xin, L.; Song, W.; Cao, Z.; and Zhang, J. 2021b. Neurolkh: Combining deep learning model with lin-kernighan-helsgaun heuristic for solving the traveling salesman problem. *Advances in Neural Information Processing Systems*, 34: 7472–7483.

Xing, Z.; and Tu, S. 2020. A graph neural network assisted monte carlo tree search approach to traveling salesman problem. *Ieee Access*, 8: 108418–108428.